ISSN 1068-3739, Russian Meteorology and Hydrology, 2017, Vol. 42, No. 10, pp. 644–652. Allerton Press, Inc., 2017.
Original Russian Text O.Yu. Antokhina, P.N. Antokhin, O.S. Zorkal'tseva, E.V. Devyatova, 2017, published in Meteorologiya i Gidrologiya, 2017, No. 10, pp. 34–45.

Atmospheric Blockings in Western Siberia. Part 1. Detection Features, Objective Criteria, and Their Comparison

O. Yu. Antokhina[a]*, P. N. Antokhin[a], O. S. Zorkal'tseva[b], and E. V. Devyatova[b]

[a]*Zuev Institute of Atmospheric Optics, Siberian Branch of Russian Academy of Sciences, pl. Academika Zueva 1, Tomsk, 634055 Russia*

[b]*Institute of Solar-Terrestrial Physics, Siberian Branch of Russian Academy of Sciences, ul. Lermontova 126a, Irkutsk, 664033 Russia*

**e-mail: olgayumarchenko@gmail.com*

Received April 19, 2016; in final form, July 4, 2016

Abstract—Based on the NCEP/NCAR and ERA-Interim reanalysis archives, we investigated different methods to detect atmospheric blocking events in Western Siberia. Two criteria were studied that are based on calculating meridional gradients of the 500 hPa height and potential temperature at the dynamic tropopause. A situation is considered blocking, when it features a gradient inversion of the investigated characteristics. Additionally, we performed a synoptic analysis of individual blocking events.

DOI: 10.3103/S106837391710003X

Keywords: Atmospheric blocking, Western Siberia, criterion of blocking

1. INTRODUCTION

Problems of atmospheric blocking have been paid increasing attention to [1, 4, 7, 9–12, 14, 16–22] every year. During atmospheric blocking, the westerly jet and eastward shift of circulation systems characteristic of the mid-latitudes are violated. Extreme weather phenomena, such as droughts in summer and extreme colds in winter, are related to blocking events. Besides temperature anomalies, blockings produce conditions for the essential redistribution of precipitations [17], gas and aerosol components of air [4, 8, 22].

Western Siberia is not a region with high atmospheric blocking frequency [10]. Nevertheless, even at low frequency, atmospheric blockings may impact weather conditions and living circumstances of people in the region. A vivid example is the episodes of winter [1] and summer blocking in 2012. In Western Siberia, June 2012 was the warmest since 1891, and December 2012 was the coldest in the history of instrumental observations [3]. So, there is an essential necessity in more detailed investigations into the variability of blocking events in the region.

At present, the Western Siberian climatic variability of the temperature and moisture regime, synoptic processes, and atmospheric gas composition has been studied in detail [5, 6, 8], but blocking variability practically has not been investigated. The results obtained generally for the Siberian-Ural region, for example in [11, 12], fill the existing gap to a certain extent. However, one cannot confidently assert that the blocking frequency variations obtained for such a vast region are equally characteristic of its separate parts.

To investigate blocking events, one uses different indices (criteria) of blocking. The main goal of any blocking index is to determine objectively the number of blocking events and their geographical position during a certain time interval. In the recent decades, not only the classical methods for blocking detection [2, 16, 20, 21] have been updated, but also new approaches [18, 19] have been developed. The possibilities, merits, and demerits of criteria of detecting blocking situations proposed at present may differ substantially for different regions. The goal of our paper is to select (based on the data from several reanalysis archives) the most suitable criterion to autodetect blockings in Western Siberia.

2. DATA AND METHODS

2.1. Detecting Blocking Events in the Atmosphere

The main task of any blocking index is to determine objectively the number of blockings and their geographic location during the certain time period. Before switching to the analysis of the existing methods, we note several important facts that are the key ones for all the criteria. In 1950 paper [20] provided a definition of the blocking process in the atmosphere for the first time. One of the basic conditions for blocking existence, according to the author, is splitting of the westerly jet into two branches that are significant in terms of airmass transport. Currently, it is considered [19] that a necessary blocking component is the presence of a large-amplitude equivalent-barotropic anticyclone poleward of the anomalous eastern jet.

Depending on the pressure field configuration, one identifies two basic types of blocking [14]: monopole and dipole. A monopole blocking looks like an intensified ridge, and there are atmospheric troughs at its foot on either side. Due to its shape, such blockings are termed "Omega" ( ). A dipole blocking in space looks like the meridionally-oriented numeral 8 comprising a blocking anticyclone and a cyclonic region. The anticyclone is from the blocking polar side, and the cyclonic part is from the equatorial side. To honor the researcher who identified this blocking type, the latter is referred to as "Rex" [14].

A number of studies deal with methods for blocking detection [2, 10–12, 16, 18–21]. Until now, there are many disputable issues, particularly, when studying blockings in certain regions. One of the detailed reviews of the existing blocking criteria is proposed in [9]. As the studied region (Western Siberia, 60 –90 E) was selected somewhat artificially in terms of atmosphere circulation features, we do not address the blocking criteria that are rather intended to calculate the blocking intensity. Using similar criteria (blocking action, block intensity) is expedient when investigating large regions, because this implies calculating the difference between the blocking anticyclone center and its periphery as well as integrating its characteristics. We constrain ourselves to comparing two criteria enabling us to establish the presence of blocking for each individual longitude. These criteria are based on calculating the gradients of meteorological characteristics on either side of the blocking central latitude ($_c$). This parameter ($_c$) is a key one in diagnosing blockings, because it reflects the region of Rossby wavebreaking [18] and is calculated by the climatic position of the storm track (eddy kinetic energy at the 300 hPa height).

The first approach was laid already in 1950s [20]. The criteria based on this approach have been developed in many studies. We select one of them proposed in [16] and updated by the present paper authors in [21]. According to [21], the following gradients are calculated:

$$\begin{aligned} \text{GHGS} &\quad \frac{Z(\ _0) \quad Z(\ _s)}{\ _0 \quad \ _s}; \\ \text{GHGN} &\quad \frac{Z(\ _n) \quad Z(\ _0)}{\ _n \quad \ _0} \end{aligned} \tag{1}$$

where Z is 500 hPa geopotential height at latitude and longitude ; $_n = 80$ N , $_0 = 60$ N , $_s =$ $= 40$ N , $= 4$.

A situation is considered blocking, when GHGS > 0, GHGN < –10 m/degree of latitude. Another (additional) condition signifies that there should be a strong western stream north of the blocking; thereby, the cases of anomalous southward shift of the mid-latitude jet stream are eliminated from "the blocking catalog."

The other used index was proposed in [18, 19]. This is the so called PV- blocking criterion based on the estimate of the atmosphere dynamic characteristics, potential vorticity (PV) and potential temperature ( ). To establish a blocking fact, one studies the variation in the potential temperature at the dynamic tropopause (PV-) relative to $_c$. In the Northern Hemisphere, the dynamic tropopause is approximated by the 2 pvu surface, 1 pvu = 10^{-6} K m^2/(kg s). The PV- index has great values for the tropical tropopause and smaller ones for the polar tropopause. As PV- (at some assumptions) may be considered as material, the investigation into its directional distribution enables us to identify not only the blocking event presence but also the origin of airmasses in the blocking surroundings as well as their transformation. To autodetect blocking, one calculates differences in the total values of potential temperature:

$$\frac{2}{\ _0} \int_{\ _0}^{\ /2} d \quad \frac{2}{\ _0} \int_{\ /2}^{\ } d \tag{2}$$

where $_0 = \ _c(\ )$, $= 4$.

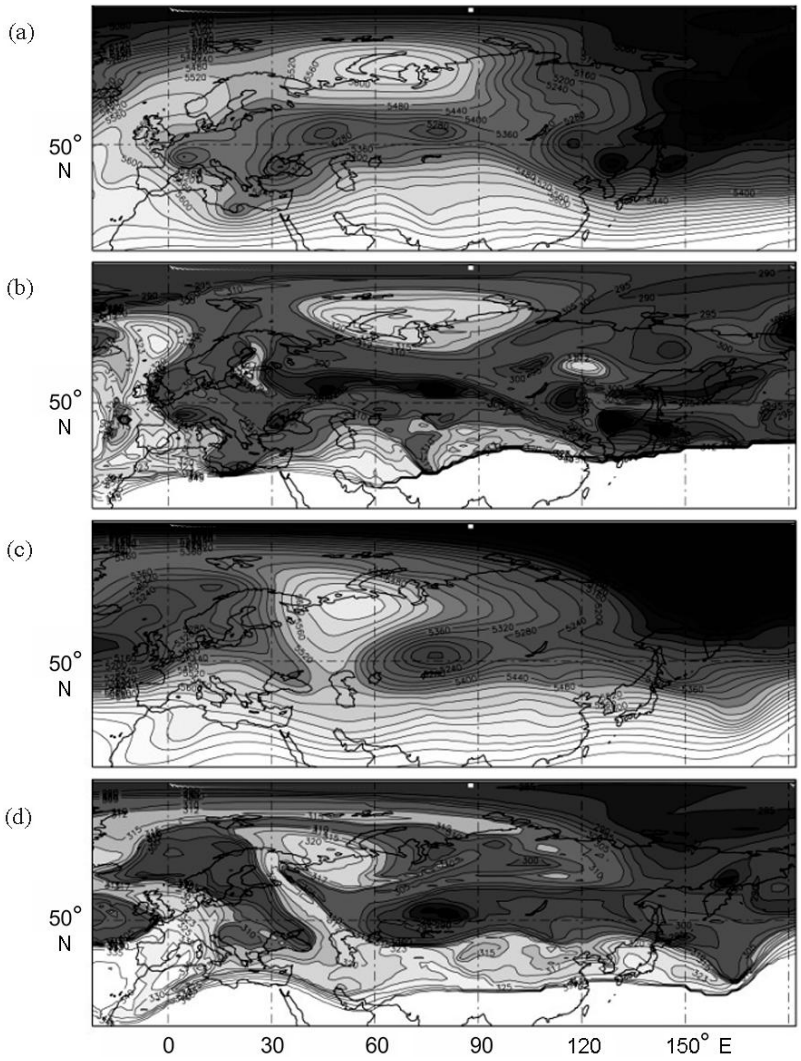

Fig. 1. Distributions of (a, c) the 500 hPa geopotential height and of (b, d) the potential temperature at the dynamic tropopause at 12:00 GMT for the blocking events on (a, b) January 31, 2012 and (c, d) December 14, 2012. The distributions are built from the ERA-Interim reanalysis data.

According to [18, 19], < 0 in the westerly jet, and > 0 in the regions with blocking.

As noted in [19], the PV- value, being a dynamic characteristic, is more sensitive than the geopotential surface height. Therefore, its spatial distribution appears more detailed. For example, Figure 1 provides Z_{500} and PV- distributions at 12:00 GMT on January 31, 2012 and December 14, 2012. One can clearly see "filaments" in the potential temperature distribution (Figs. 1b and 1d) that reflect airmasses of different origin. Apparently, the PV- value "motley" distribution elucidates the selection of a sufficiently wide band for the $= 30$ integration, instead of selecting simply several values in certain regions, like for the GHGS criterion.

A more fundamental difference for the addressed criteria is selecting the $_c$ value. When calculating the GHGS criterion in the Northern Hemisphere for all longitudes it is assurred that, $_c = 50$ N ($_{50}$). To calculate , [19] proposed another approach to determine $_c$. Based on the analysis of a large dataset, it was shown that the climatic position of the storm track differs significantly in different longitudinal sectors. Therefore, when calculating , the authors of [19] used the latitude that changes depending on the longitude. Such an approach helped to obtain an essential decrease in the blocking frequency in the west of the Pacific Ocean, as compared with the application of the fixed latitude $_{50}$. According to the calculations in [18, 19], in Western Siberia $_c$ is approximately 8 to the north of $_{50}$. The number of the blockings detected in Western Siberia obtained in the calculations by applying increases by several times. Additionally, the blocking frequency

Table 1. Mean blocking frequency (%) in Western Siberia in 1979–2014

Parameter	50				50			
	GHGS	GHGS + GHGN	GHGS	GHGS + GHGN		+ GHGN		+ GHGN
				Instantaneous blocking				
F								
NCEP/NCAR	5.73	5.49	13.15	8.24	–	–	–	–
ERA-Interim	5.79	5.51	13.44	8.52	12.61	10.96	22.89	12.38
F	5	0	142	52	129	99	316	125
				Blockings longer than five days				
NCEP/NCAR	2.42	2.23	6.02	3.22	–	–	–	–
ERA-Interim	2.29	2.08	5.79	3.09	2.33	1.90	6.16	2.56
F	9	0	174	47	12	–9	196	23

minimum obtained near 90° E (when calculating with $_c = 50$ N), shifts eastward, into the 135 E region. With account of such fundamental differences in the number of the detected Western Siberian blockings, the estimate of justifying the use for the investigated territory was especially relevant. Therefore, we calculated the blocking frequency for both criteria by applying and $_{50}$.

Also, it was interesting to determine how the role of the GHGN condition changes when blocking is autodetected by applying $_{50}$ and . When calculating the criteria with , it was necessary to change the parameters of the additional GHGN condition. Since in Western Siberia the blocking central latitude shifts by 8 on average, we considered expedient to use the following parameters: $_n = 85$ N , $_0 = 65$ N . The parameter depending on the scale of the used grid played an important role in selecting these indicators.

In our study all the blockings are categorized into instantaneous blockings (IBs) and 5-day (and longer) blockings (B5). According to [19], the situations corresponding to the above criteria over at least one observational interval were included in the first category. Further in the paper, we add $_{50}$ to the name of the criterion calculated by using the standard blocking latitude, whereas is added to the name of the criterion calculated by using the "floating" latitude.

2.2. Calculating the Blocking Frequency

We calculated the blocking event frequency in percentage. The product of days in a year ($t = 365$ or 366) and the number of grid points ($l = 13$) within the 60 –90 E range at the 2.5 grid step is taken as 100% (the greatest possible number of realizations). The IB frequency was calculated as the ratio of the number of cases meeting the blocking conditions to the greatest possible number of all realizations within the indicated range. The B5 frequency was calculated as the ratio of the total of the blocking days (with 5-day and longer blockings) to the greatest possible number of realizations. For our study we use the data from two reanalysis archives: NCEP/NCAR [15] (Z_{500}) and ERA-Interim [13] (Z_{500}, PV-). All the data have the 2.5° spatial resolution; thus, is 5 . When calculating by formulae (1) and (2), we selected the maximum value of five (5 , 2.5 , 0) for all the parameters.

3. RESULTS

3.1. Mean Blocking Frequency

Table 1 presents the results of calculating the mean blocking frequency (F) in Western Siberia (IB and B5) over 1979–2014. The F value was calculated as follows:

$$F \quad \frac{F}{F_b} \quad 1 \quad 100\% \qquad (3)$$

Table 2. Correlation coefficients for the blocking criteria in Western Siberia to the base criterion over 1979–2014

Blocking	50			50			
	GHGS	GHGS	GHGS + GHGN		+ GHGN		+ GHGN
IB	0.99	0.45	0.73	0.76	0.75	0.16	0.54
B5	0.99	0.45	0.70	0.74	0.69	0.29	0.51

where F_b is the blocking frequency determined by the basic criterion, for which we accept GHGS($_{50}$) + + GHGN($_{50}$), and F are the blocking frequency values determined by any other criterion. We selected the basic criterion in favor of the criterion with the least blocking frequency.

Table 1 provides the mean F values for two archives. Apparently, the results obtained for different reanalysis archives agree well. However, the results obtained for different criteria differ substantially. First of all, one should focus on the following aspects of applying different blocking characteristics and different versions of determining the central latitude:

1. A change in the central blocking latitude leads to an increase in the number of the detected blockings for both considered criteria. Herewith, the correlation coefficients (Table 2) for the basic criterion and for the criteria with are insignificant. This implies that the criteria with record the situations that the criteria with $_{50}$ do not detect at all. If the criteria with detected the same events as the criteria with $_{50}$ but for a more extended interval, such an increase in frequency would not lead to an abrupt decrease in the correlation coefficients, particularly, for the ( ) criterion.

2. Addition of the GHGN condition does not play a significant role for the criteria with $_{50}$, particularly, for GHGS($_{50}$). For this criterion, eliminating the situations of the strong southward shift of the jet stream showed only 5 and 9% of similar cases of the total number for IBs and B5s, respectively. The account for the GHGN( ) condition leads to an essential decrease in the number of the detected blockings, but in this case their relation to the basic criterion increases notably (Table 2). The revealed fact may evidence that the criteria with identify much more situations for whose elimination GHGN was developed. Nevertheless, even after accounting for the GHGN condition, the number of the blockings detected by the criteria with remains more than that detected by the criteria with $_{50}$. Herewith, for the ( ) criterion, the calculation results are much more ambiguous than those for GHGS.

3. Table 1 shows that for the GHGS indicator only about half of the blocking cases are long-term B5 events ("true" blockings), whereas the remaining part of the gradient reversal situations represents a separate class of phenomena that have been less studied by now. Therefore, one may have expected the ratio between these two blocking types to probably change at the $_c$ variation. It appeared, however, that the differences for the GHGS indicator are insignificant (particularly, when accounting for the GHGN condition), i.e., the $_c$ variation simultaneously leads to an increase in the number of both long-term events and "instantaneous" blockings. Quite different situation is observed for the criterion. However, as the differences for this criterion in detecting B5s and IBs are not only in the $_c$ variation, below we discuss in greater detail the usage of the criterion to detect blocking events.

4. The correlation coefficients for the ($_{50}$) criterion and for GHGS ($_{50}$) are sufficiently great (Table 2), which evidences in favor of preferential identification of the same events by these criteria. There are, however, essential differences in detecting IB and B5 blockings through , simultaneously both for ($_{50}$) and for ( ). The number of IBs detected by the criterion is essentially more than that for the basic criterion; for long-term B5 events, particularly accounting for the GHGN condition, this difference is not significant (Table 1). Differences in detecting IBs and B5s through are especially clear as compared with the already described GHGS criterion (for which the deviation from the basic criterion is constant both for IB and for B5).

This implies that the criterion, being more sensitive, enables one to identify more short-term events of the PV- gradient reversal. As noted above, one should perform a more detailed analysis of these events. In Fig. 2 we provided the Z_{500} and PV- distributions for the situations when only ($_{50}$,) meets the blocking condition of all the used criteria. Herewith, the GHGN condition is satisfied in both cases. On the Z_{500} distribution map, in the former case (February 6, 2001, Fig. 2a) one can see a blocking near the western boundary of the investigated region, but the blocking practically does not affect Western Siberia. At the same time, if one examines the PV- distribution (Fig. 2b), a blocking is recorded throughout the entire

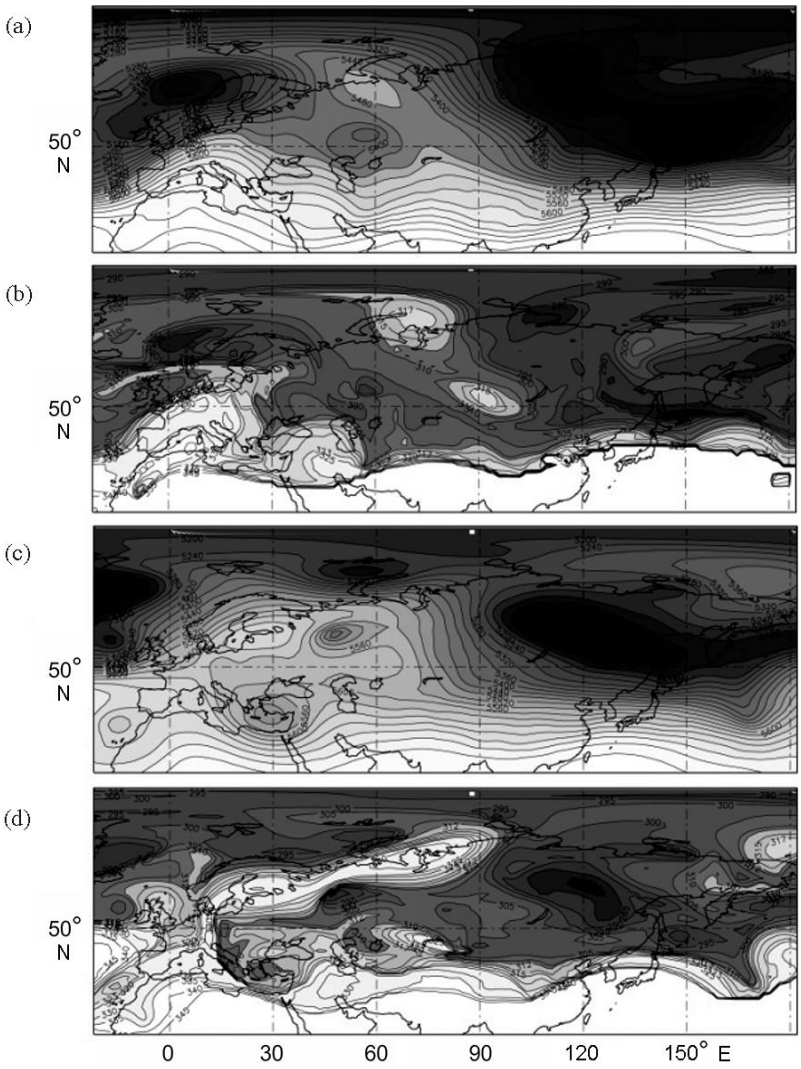

Fig. 2. The same as in Fig. 1, but for the blocking events on (a, b) February 6, 2001 and (c, d) December 3, 2001.

60°–90° E. In the latter case (December 3, 2001) in the Z_{500} field over Western Siberia there is no blocking anticyclone (Fig. 2c), but the PV- distribution (Fig. 2d) evidences the contrary situation.

The greatest values are within the region where the GHGS($_{50}$) > 0 and the GHGN($_{50}$) < –10 conditions are met (the figure is not presented). Judging by the above examples, inclusion of the remaining part of the > 0 values in automatic blocking recording remains in doubt so far.

3.2. Analysis of Individual Blocking Events

To clarify the reasons for a greater number of the blocking events detected by the criteria with the more northern blocking latitude ( ), as to well as elucidate the roles of the GHGN condition for similar events, we address the features of detecting blocking events for one of the most contrasting intervals, the year 2001. When calculating the IB frequency with no account for GHGN, it appeared that for the criteria with the number of the detected blockings is more than that for the criteria with $_{50}$ by a factor of 4 and 2 for GHGS and , respectively. The analysis of the longitude-time section of the detected events (the figure is not presented) showed that the greatest differences are in summer.

Let us address individual blocking cases recorded only by the criteria with . To begin with, we focus on the events at which GHGS( ) and ( ) showed the blocking presence, but the GHGN condition was not met (Figs. 3a–3d). One can see in the figures that over the Western Siberia, in fact, there is a situation of reversal of the Z_{500} meridional gradient (Figs. 3a and 3c) and of PV- (Figs. 3b and 3d), but the sign reversal

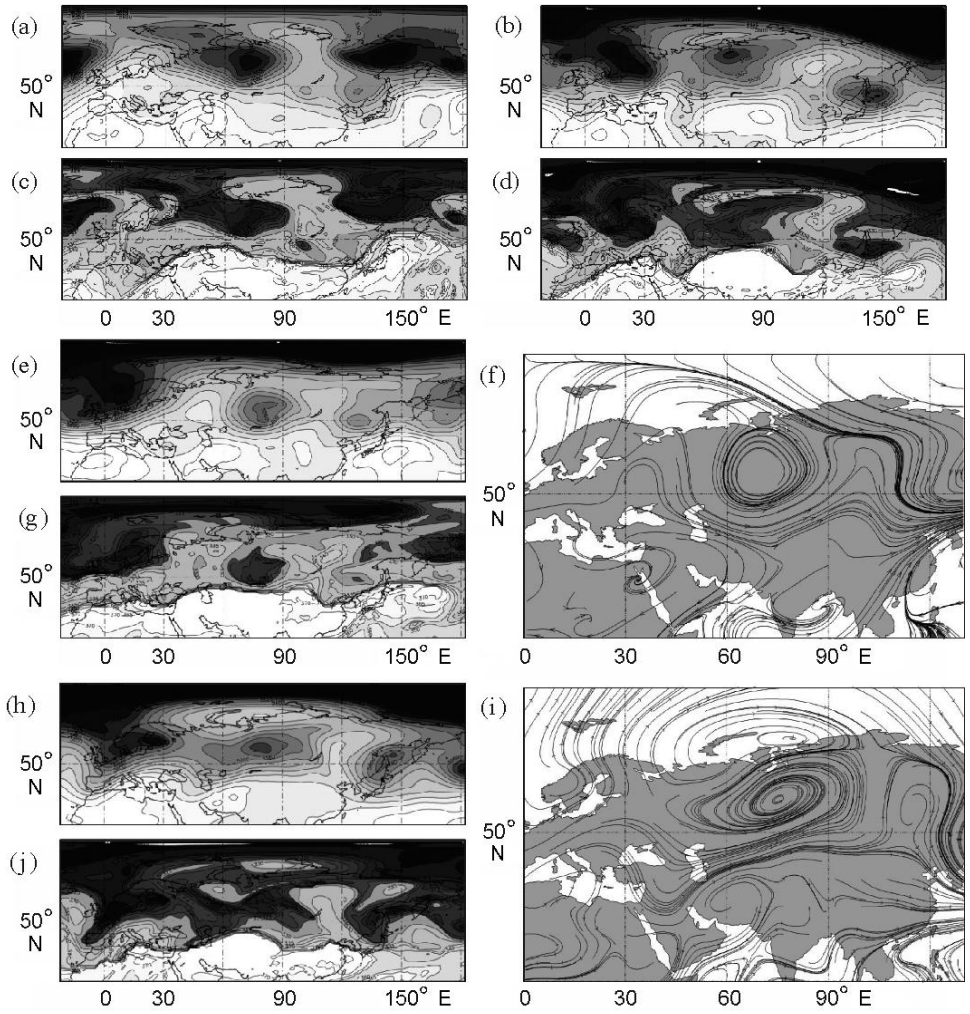

Fig. 3. Distribution of the (a, b, e, h) 500 hPa geopotential height and of the (c, d, g, j) potential temperature at the dynamic tropopause at 12:00 GMT; (f, i) the stream lines at 850 hPa for the blocking events on (a, c) August 22, 2001, (b, d) June 12, 2001, (e, f, g) July 13, 2001, and (h, i, j) June 10, 2001. The distributions are built from the ERA-Interim reanalysis data.

of these values occurs because of the deep intrusion of a tropospheric trough from the northwest. Thereof, the pressure in the southern regions of Western Siberia appears higher than that in the northern regions, calculation of the GHGS( ) and ( ) criteria evidences the blocking presence over Western Siberia, but the blocking is not observed in fact. The synoptic analysis of pressure and isentropic fields over the entire observational interval in the cases when only the criteria with met the blocking condition, showed that there are many similar situations for the Western Siberia territory in the summertime. Unfortunately, it is impossible to consider even their small part within one paper. However, we assume that it is these cases that cause an essential increase in the number of blockings over Western Siberia illustrated in the plot of the mean blocking frequency in [18, 19]. Although these synoptic formations may be sufficiently stable (as many as five days and more) and their frequency for Western Siberia is sufficiently great, they cannot be attributed to blocking events in the calculations of a long-time variability due to the absence of a large-scale barotropic anticyclone over the region. One might assume that with the account for the GHGN additional condition it would be possible to avoid recording the situations described above. However, it appeared that there is also a probability to detect "cutoff cyclones" when observing the GHGN condition. The distributions in Figs. 3e–3g demonstrate a region of a "cutoff" low pressure over Western Siberia, whereas the criteria with identify it as a blocking. At the same time, the GHGN condition is met, because there is a sufficiently strong westerly jet over the low pressure region (Fig. 3f).

There are also such configurations of the 500 hPa height field for which the GHGS($_{50}$) criterion does not detect blocking over Western Siberia due to a strong northward shift of the blocking anticyclone. The criteria with also record such cases, and the GHGN condition is met in this case. The situation in Figs. 3h–3j may be an example: from the streamline configuration (Fig. 3i) one can see that the situation is, in fact, blocking, but due to the extreme north position, the GHGS($_{50}$) criterion does not detect a similar situation. It is important to note that in this case the duration of the described situation is not too long (June 9 and 10). Already on June 11 over Western Siberia the situation was observed with the cutoff low described above.

4. CONCLUSION

Thus, the analysis showed that the results of calculating the blocking event frequency for the two reanalysis archives appeared to agree well among themselves. However, for the different criteria and methods of setting the blocking central latitude, the number of blockings detected in Western Siberia differs significantly. The criterion calculated based on PV- was established to be more sensitive to atmospheric variations, and it detects such weak gradient reversals that often do not manifest themselves in the 500 hPa field. However, the synoptic analysis of individual cases showed that these reversals may not often evolve to the blocking state. The PV- gradient greatest values agree with the region where the Z_{500} gradient values meet the blocking condition, i.e., the efficiency of the addressed criteria is comparable for the most evolved blocking situations.

Detecting blockings by calculating the PV- gradients, as well as by using , is a too subtle and ambiguous instrument that requires involving a synoptic analysis. However, calculating PV- and may be useful when analyzing individual events in detail, thus improving the insight into the dynamic processes occurring in the atmosphere during blockings. To autodetect blockings in Western Siberia the criterion based on calculating the Z_{500} gradients with applying the fixed central $_{50}$ blocking latitude is more appropriate.

ACKNOWLEDGMENTS

This research was supported by the Russian Foundation for Basic Research (grants No. 17-05-00119 and 17-05-00374), by the Russian Academy of Sciences Presidium (Program No. IX.135-6) “Study of Air Composition Changes Governing Dynamics of Radiation-important Properties of the Atmosphere over Siberia,” by the Program of Fundamental Scientific Research of the Siberian Branch of the Russian Academy of Sciences No. II.2P “Integration and Development” 2017.

REFERENCES

1. A. D. Golubev, A. M. Kabak, N. A. Nikol’skaya, et al., “Westerly Jet Blocking during 2012 Winter over Eurasia and Related Weather Anomalies,” Trudy Gidrometcentra Rossii, No. 349 (2013) [in Russian].
2. G. V. Gruza and L. V. Korovkina, “Climatic Monitoring of Western Transfer Blocking in the Northern Hemisphere,” Meteorol. Gidrol., No. 8 (1991) [Sov. Meteorol. and Hydrol., No. 8 (1991)].
3. *Report on Climatic Features over Russian Federation Area in 2012* (M., 2013) [in Russian].
4. N. F. Elansky, I. I. Mokhov, I. B. Belikov, et al., “Gas Admixture in the Atmosphere over Moscow in Summer 2010,” Izv. Akad. Nauk, Fiz. Atmos. Okeana, No. 6, **47** (2011) [in Russian].
5. I. I. Ippolitov, M. V. Kabanov, S. V. Loginov, et al., “Variability of the Thermal Balance Components of the Earth Surface over Russian Asia in the Recent Global Warming Period,” Optika Atmos. Okeana, No. 1, **24** (2011) [in Russian].
6. I. I. Ippolitov, S. V. Loginov, E. V. Kharutkina, et al., “Climatic Variability over Asian Part of Russia in the 1975–2012,” Geografiya i Prirodnye Resursy, No. 4, **35** (2014) [in Russian].
7. I. I. Mokhov, “Abnormal Summer 2010 in the Context of General Climate Changes and Its Anomalies,” in *Analysis of the Anomalous Weather Conditions over Russia in Summer 2010*, Ed. by N. P. Shakina (M., Triada LTD, 2011) [in Russian].
8. T. K. Sklyadneva, B. D. Belan, and M. Yu. Arshinov, “Radiation Regime in Tomsk under Smoke Haze Conditions,” Optika Atmos. Okeana, No. 3, **28** (2015) [in Russian].
9. N. P. Shakina and A. R. Ivanova, “The Blocking Anticyclones: The State of Studies and Forecasting,” Meteorol. Gidrol., No. 11 (2010) [Russ. Meteorol. Hydrol., No. 11, **35** (2010)].
10. D. Barriopedro, R. Garcia-Herrera, A. R. Lupo, and E. A. Hernandez, “A Climatology of Northern Hemisphere Blocking,” J. Climate, **19** (2006).

11. H. N. Cheung, W. Zhou, H. Y. Mok, et al., "Revisiting the Climatology of Atmospheric Blocking in the Northern Hemisphere," Adv. Atmos. Sci., No. 2, **30** (2013).
12. H. N. Cheung, W. Zhou, Y. Shao, et al., "Observational Climatology and Characteristics of Wintertime Atmospheric Blocking over Ural–Siberia," Climate Dyn., No. 1, **41** (2012).
13. D. P. Dee et al., "The ERA-Interim Reanalysis: Configuration and Performance of the Data Assimilation System," Quart. J. Roy. Meteorol. Soc., No. 656, **137** (2011).
14. F. Huang, X. Tang, S. Y. Lou, and C. Lu, "Evolution of Dipole-type Blocking Life Cycles: Analytical Diagnoses and Observations," J. Atmos. Sci., **64** (2007).
15. E. Kalnay, M. Kanamitsu, and R. Kistler, "The NCEP/NCAR 40-year Reanalysis Project," Bull. Amer. Meteorol. Soc., No. 3, **77** (1996).
16. H. Lejenas and H. Oakland, "Characteristics of Northern Hemisphere Blocking as Determined from Long Time Series of Observational Data," Tellus A, **35** (1983).
17. Y.-J. Park and J.-B. Ahn, "Characteristics of Atmospheric Circulation over East Asia Associated with Summer Blocking," J. Geophys. Res. Atmos., **119** (2014).
18. J. L. Pelly, *Predictability of Atmospheric Blocking*, A thesis submitted for the degree of Doctor of Philosophy (2001).
19. J. L. Pelly and B. J. Hoskins, "A New Perspective on Blocking," J. Atmos. Sci., No. 3, **60** (2003).
20. D. F. Rex, "Blocking Action in the Middle Troposphere and Its Effect upon Regional Climate. I. An Aerological Study of Blocking Action," Tellus, **2** (1950).
21. S. Tibaldi and F. Molteni, "On the Operational Predictability of Blocking," Tellus A, **42** (1990).
22. M. Tressol, C. Ordonez, R. Zbinden, et al., "Air Pollution during the 2003 European Heat Wave as Seen by MOZAIC Airliners," Atmos. Chem. Phys., **8** (2008).